Supporting Information

Possible bond character effect on self-healing properties of materials for sustainable energy conversion

Yuval Mualem[1,2], David Cahen[3], Yevgeny Rakita[4*], Hannah-Noa Barad[1,2*]

[1] Department of Chemistry, and Institute of Nanotechnology & Advanced Materials (BINA), Bar-Ilan University, 5290002 Ramat-Gan, Israel

[2] Israel National Institute of Energy Storage (INIES), Ramat-Gan 5290002, Israel

[3] Department of Molecular Chemistry & Materials Science, Weizmann Institute of Science, Rehovot 7610001, Israel

[4] Department of Materials Engineering, Ben Gurion University of the Negev, Be'er Sheva 8410501, Israel

Section 1: Definition of Relative Structural Polarization

Every material, under perturbation of an external electric field, will experience displacement of both ions and electrons, that will oppose the applied field. The total polarization that opposes an applied electric field, $\vec{E}$, will be proportional to the induced polarization density, $\vec{P}$, which is the sum of dipole moments normalized to volume. Between every two atoms i and j we can write the dipole moment, $\vec{p}$, and the polarization vector, $\vec{P}$, as:

$$\vec{p} = q_{ij} \cdot r_{ij} \qquad (Eq.1)$$

$$\vec{P} = \rho \cdot \sum_i \vec{p}_i \qquad (Eq.2)$$

where q_{ij} , $r_{ij,}$ and ρ are the magnitude of the charge separation, the distance between the charges, and the volume density, respectively. Assuming an oscillating perturbation, the polarization at frequency $\omega, \vec{P}(\omega)$, will then be:

$$P\ \omega\ = \varepsilon_0 \chi_r\ \omega\ E\ w\ = \varepsilon_0\ \varepsilon_r\ \omega\ - 1\ \cdot E\ w \qquad Eq.3$$

where ε_0, ε_r, and χ_r are the vacuum permittivity, relative permittivity, and the electric susceptibility, respectively. The charge displacement with frequency, $\vec{D}(\omega)$, can then be written as:[1]

$$\vec{D}(\omega) = \varepsilon_0 \vec{E}(\omega) + \vec{P}(\omega) = \varepsilon_0 \varepsilon_r(\omega) \vec{E}(\omega) \qquad (Eq.4)$$

Now let us consider the total 'polarizable' charges in bonds and bonded atoms, and separate them into the electronic and structural (atomic) contributions. At different frequencies ω of the perturbing electric field, one may expect changes in the average total charge density between neighboring atoms by $\mathrm{d}(\mathrm{q_{ij}})$ or a change in the average inter-atomic distance by $\mathrm{d}(\mathrm{r_{ij}})$. If we consider the same magnitude of the applied electric field but at different frequencies, the polarizability of each component should vary. At sufficiently high frequencies (typically at the THz range or above; noted as '∞'), the perturbing alternating field is faster than the nuclei motion, so we can write*:*

$$\frac{d\vec{D}\ \infty}{\vec{E}} = \frac{d\vec{D}_{elec}}{\vec{E}}\ =\ \varepsilon_0 \varepsilon_r\ \infty \qquad Eq.5$$

At low frequencies (noted as 's' for 'static'), where atomic motion is much faster than the depolarization field, we can write:

$$\frac{d\vec{D}(0)}{\vec{E}} = \frac{d\vec{D}_{elec} + d\vec{D}_{atom}}{\vec{E}}\ =\ \varepsilon_0 \varepsilon_r(s) \qquad (Eq.6)$$

Considering the ratio between the polarization-displacements at $\omega \to \infty$ and $\omega \to 0$, we can write:

$$\frac{d\vec{D}(0)}{d\vec{D}(\infty)} = \frac{d\vec{D}_{elec} + d\vec{D}_{atom}}{d\vec{D}_{elec}} = 1 + \frac{d\vec{D}_{atom}}{d\vec{D}_{elec}} = \frac{\varepsilon_r(s)}{\varepsilon_r(\infty)} \qquad (Eq.7)$$

If we define the displacement due to the ***relative structural polarization (RSP)***, as RSP $\equiv \frac{d\vec{D}_{atom}}{d\vec{D}_{elec}}$, then:

$$\boldsymbol{RSP \equiv \frac{d\vec{D}_{atom}}{d\vec{D}_{elec}} = \frac{\varepsilon_r(s)}{\varepsilon_r(\infty)} - 1} \qquad (Eq.8)$$

To understand RSP more intuitively, we consider a boundary condition of a purely monovalent ionic system (pure ionic bonding). We can assume that at low frequencies the ionic and electronic contributions are energetically equal, so that the electrostatic displacement energy is equally split between the electronic and atomic parts, meaning, $d\vec{D}_{elec} = d\vec{D}_{atom}$. If this is the case, for purely ionic materials RSP≈1. The less ionic the bond (more covalent), then, energetically, depolarization effects will favor electronic over structural displacement, *i.e.*, $d\vec{D}_{elec} > d\vec{D}_{atom}$, making RSP < 1. If there is a repulsive covalent contribution to the bonding, then, energetically, depolarization effects will favor atomic displacement to reduce the anti-bonding energetic penalty by displacing atoms. Thus, for anti-bonding covalency $d\vec{D}_{elec} < d\vec{D}_{atom}$, making RSP > 1. These trends were demonstrated by Rakita et al..[2]

Section 2: RSP experimental and computed values

As discussed in the main text, several discrepancies were found between the computed RSP values from MP and the experimental values found in the literature. Here we present 6 figures (S1-S6) which correspond to Figures 2b-g from the main text to show the experimental and computed RSP points and see how it affects the observed results. In all those figures, the experimental results are marked by X and the computed by O. In these figures we see no clear discrepancy that can raise a doubt on our findings.

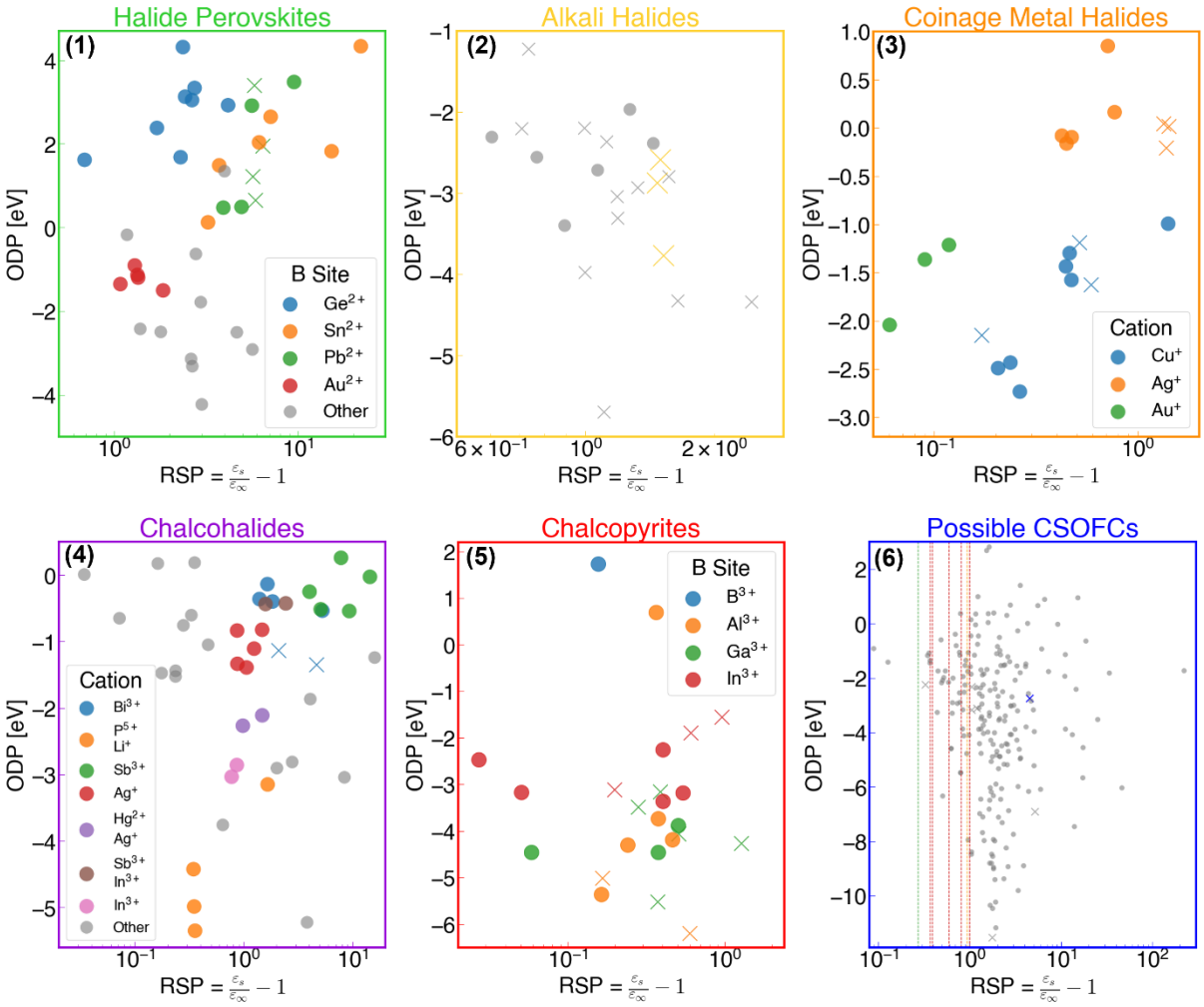

Figure S1-S6. The plots in Figure 3b-g with circle as computed RSP entries and X as experimental RSP entries. The materials groups correspond to Figure 3b-g, as follows: (1) Halide Perovskites (green) (2) Alkali Halides (yellow) (3) Coinage Halides (orange) (4) Chalcohalides (purple) (5) Chalcopyrites (red) (6) Possible CSOFCs (blue).

In the chalcopyrties group, a clear underestimation of RSP values by Materials Project was observed. This can be seen in a computed-measured values comparison plot in Figure S7. This large discrepancy can arise from the anisotropy of the pyrites and their trigonal symmetry, which may not be well accounted for in the RSP calculations.

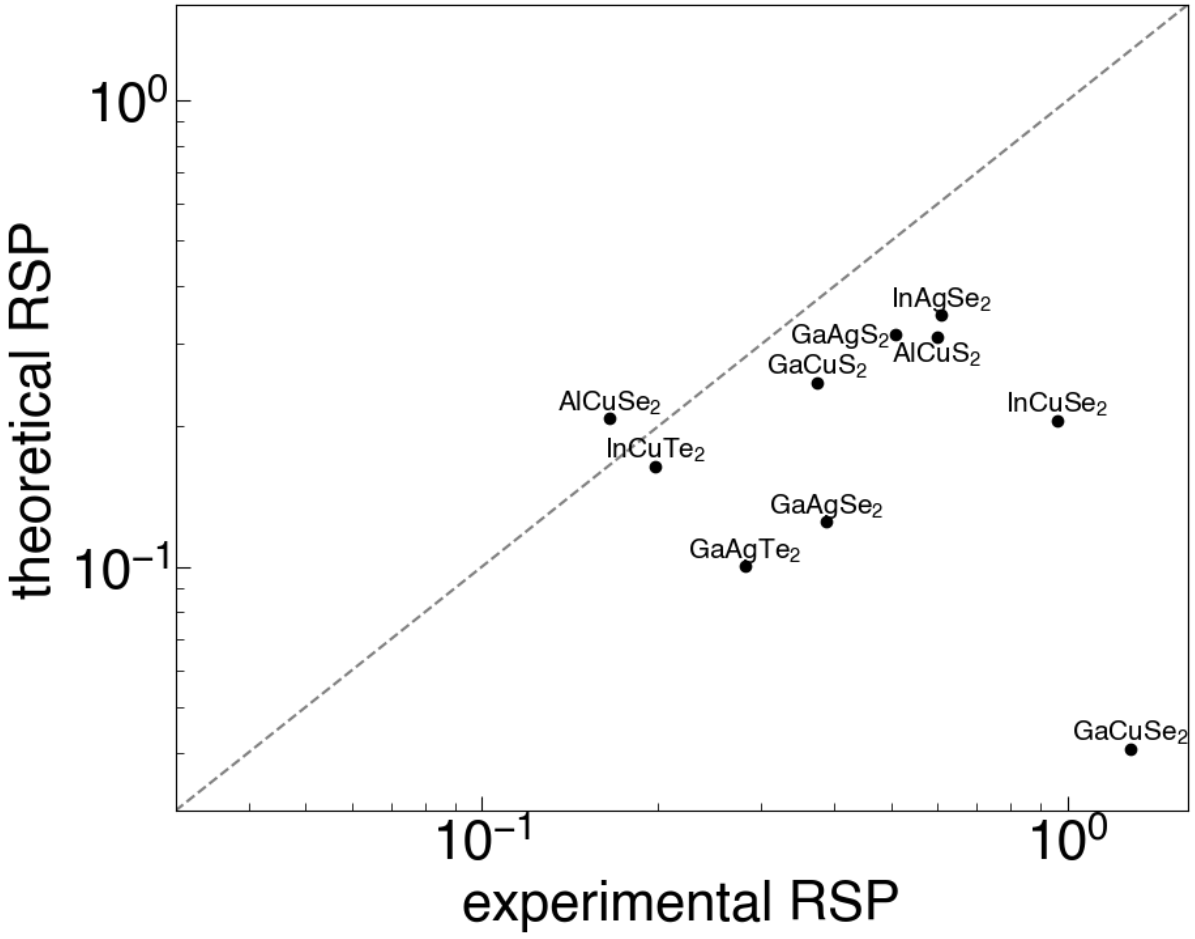

Figure S7: Comparison plot between measured RSP values (‘experimental’) and computed RSP values (‘theoretical’) of the chalcopyrites group. The grey dotted line is a symmetry line.

Considering the peculiarity of the CSOFCs case, having RSP > 1 for most of the group, we further investigate the RSP values to disprove any computational effect on the results. In Figure S8 a trend of the ionic component against the RSP is plotted for values from MP and experimental for all oxides in the database. It is clear from here the spread of the values, both the ionic component and the RSP, is about the same in both types of data. Thus, we assume no computation effect is apparent in this case, in contrast to the chalcopyrites case.

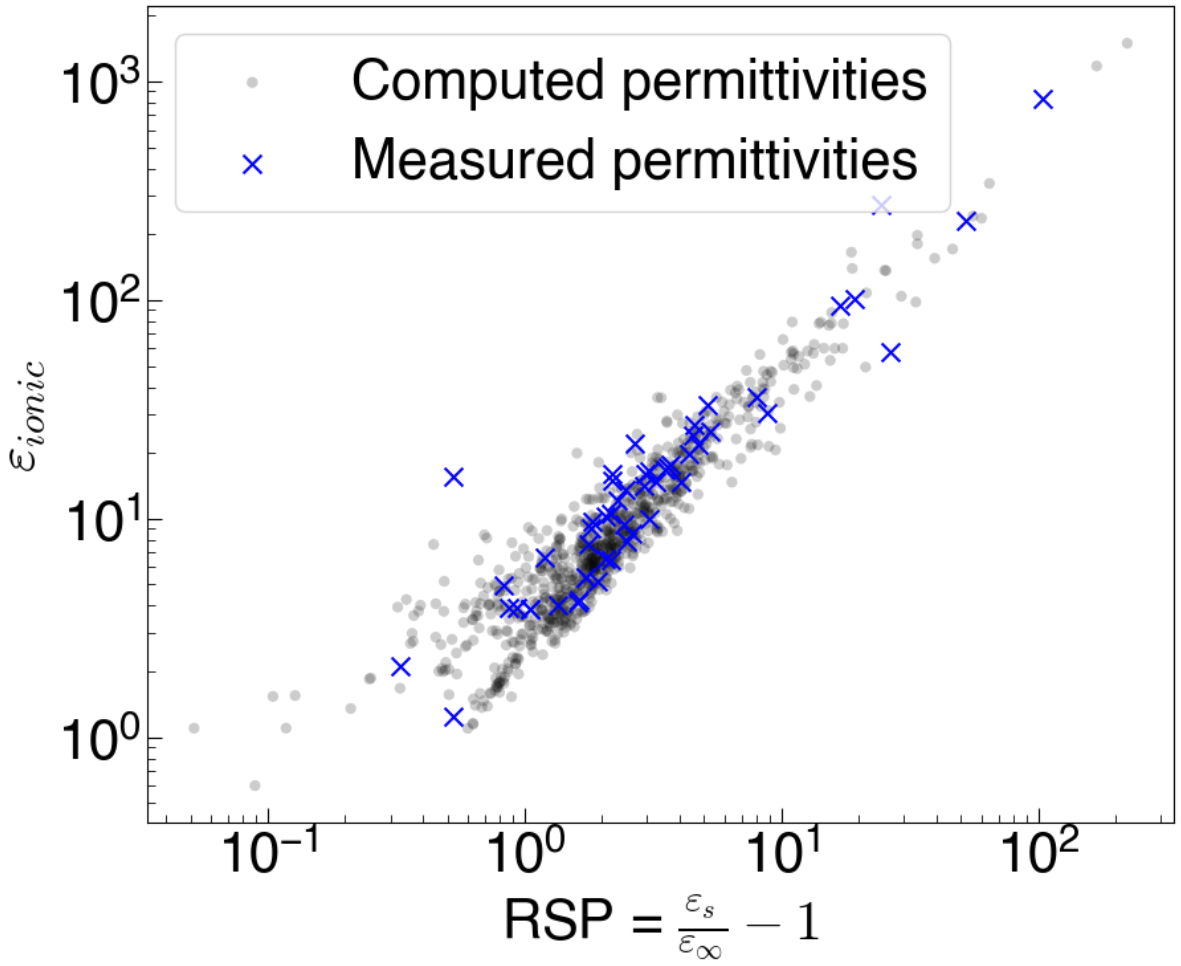

Figure S7. Correlation between the RSP value and the ionic permittivity value for all the oxides. Black circles correspond to calculated values and blue X to measured ones.

Section 3: Selected datapoints

The material groups were defined as follows:

1. Halide perovskites: halides with formula ABX_3 and octahedral coordination.
2. Alkali halides: halides with an alkali cation and FCC crystal structure (space group 225).
3. Coinage halides: halides with Ag, Cu or Au cation.
4. Chalcohalides: materials with halide and chalcogenide as anions.
5. Complex Pyrites: materials with the formula ABX_2 where either A = Ag, Cu and B = B, Al, Ga, In, and X is a chalcogenide, or pnictide pyrites, where A = Zn, Cd and B = Si, Ge, Sn, and X is a pnictide.
6. Possible Ceramics for SOFCs: Defined according to E_{vac} = oxygen vacancy formation energy, taken from Baldassari et al..[3] If 2 eV < E_{vac} < 5 eV then an oxide is included in this set, following the ranges defined by Baldassari et al.. In multinary oxides, each atom's binary oxide E_{vac} is evaluated, and then a weighted average (according to stoichiometric ratios) is taken.

The tables S1-S8 are found in the excel file Supporting_Tables.xlsx.

Table S1: The entire dataset

Table S2: Halide Perovskites data points

Table S3: Alkali Halides data points

Table S4: Coinage Halides data points

Table S5: Chalcohalides data points

Table S6: Complex Pyrites data points

Table S7: Possible ceramics for solid oxide fuel cells (CSOFCs) data points

Table S8: Training data points for classification ML model

Bibliography

1. Griffiths, D.J. (2017). Introduction to Electrodynamics 4th ed. (Cambridge University Press).

2. Rakita, Y., Kirchartz, T., Hodes, G., and Cahen, D. (2019). Type and Degree of Covalence: Empirical Derivation and Implications. Preprint at arXiv, https://doi.org/10.48550/arXiv.1907.03971 https://doi.org/10.48550/arXiv.1907.03971.

3. Baldassarri, B., He, J., Gopakumar, A., Griesemer, S., Salgado-Casanova, A.J.A., Liu, T.-C., Torrisi, S.B., and Wolverton, C. (2023). Oxygen Vacancy Formation Energy in Metal Oxides: High-Throughput Computational Studies and Machine-Learning Predictions. Chem. Mater. *35*, 10619–10634. https://doi.org/10.1021/acs.chemmater.3c02251.